

# All-optical flip flop based on a symmetric Mach-Zehnder switch with a feedback loop and multiple forward set/reset signals

H. Le Minh, Z. Ghassemlooy, and Wai Pang Ng  
 Northumbria University, School of Computing, Engineering and Information Sciences, Optical Communications Research Group, Newcastle upon Tyne, NE1 8ST, United Kingdom  
 E-mail: h.le-minh@unn.ac.uk

**Abstract.** A novel all-optical set/reset flip flop (AOFF) based on a symmetric Mach-Zehnder switch with a feedback loop and multiple forward set/reset signals is presented. The proposed flip flop has a fast response, a flat output gain, and a short switching-on interval of a few hundreds of picoseconds regardless of the associated feedback-loop delay. It is shown that a high on/off contrast ratio at the AOFF output is achieved above 20 dB. © 2007 Society of Photo-Optical Instrumentation Engineers.  
 [DOI: 10.1117/1.2721773]

Subject terms: all-optical flip flop; symmetric Mach-Zehnder switch; feedback loop.

Paper 060880L received Nov. 8, 2006; accepted for publication Jan. 10, 2007; published online Apr. 24, 2007.

## 1 Introduction

An all-optical flip flop (AOFF) is an essential component for latching functions in high-speed all-optical processing applications.<sup>1,2</sup> Currently, an AOFF can be realized using the coupled multimode-interference bistable laser diodes scheme<sup>3,4</sup> or by a symmetric Mach-Zehnder (SMZ) switch with a single-pulse counter-propagation control-signal feedback loop.<sup>5</sup> In the former scheme, a number of wavelengths are required; whereas in the latter scheme, only a single wavelength is employed with a feedback loop (FBL) to enhance the AOFF configuration simplicity. Because the real-time signal-propagation delay associated with the FBL is hundreds of picoseconds,<sup>5</sup> there is a lag in feedback signal (i.e., requiring a sufficient transient time equivalent to the FBL delay to fully set the AOFF in an on state) when switching the AOFF to the on state. In addition, the counterpropagation between a control and input signal in the SMZ will result in an additional delay in the rising and falling edges of AOFF output.<sup>6</sup> As a result, these proposed AOFFs operate on the order of nanoseconds. Therefore, achieving a fast response time and an on interval that is shorter than the transient time are the issues in FBL-based AOFF employed in high-speed applications. Here, we propose a new AOFF configuration assisted by a FBL SMZ with multiple forward-control signals (set *S* and reset *R*) to overcome these limitations.

## 2 AOFF Operation

An AOFF circuit block diagram and its operation principle are depicted in Fig. 1. The AOFF is composed of a SMZ switch<sup>5,7</sup> with a continuous-wave (cw) signal input; set and reset control inputs in the upper and lower control arms, respectively; and a FBL (with a signal propagation delay of  $T_{FBL}$ ) feeding  $\beta\%$  of power from the AOFF output ( $Q$ ) to the upper control arm of the SMZ. Polarization controllers are used to introduce an orthogonal polarization between the cw and control signals, and consequently, a polarization beamsplitter is used at the output of the SMZ to separate them. In the absence of the optical pulses at control inputs, and providing that both semiconductor optical amplifiers (SOAs) are identical, the SMZ is in a balance state because the signal gain and phase profiles in both arms in the SMZ are the same; thus, the cw signal propagating in both arms will not emerge at the AOFF output (i.e., in the off state). A single set pulse will pass through a number of paths with different delays and attenuators to produce a multiplexed pulse set *S* in  $T_{FBL}$ , before being applied to the upper control input of the SMZ for toggling the AOFF to the on state. The first pulse of *S* will saturate SOA<sub>1</sub>, thus inducing an imbalance in gain and phase profiles between two arms and hence causing a switching cw signal to *Q*. To maintain the AOFF in the on state, i.e., a flat SOA gain saturation level, a portion  $\beta\%$  of *Q* output power  $P_{FBL}$  is fed back to the upper control input of the SMZ. However, since  $P_{FBL}$  takes a  $T_{FBL}$  to arrive at SOA<sub>1</sub>, *S* pulses following the first pulse continue to maintain the SOA<sub>1</sub> saturation, thus precluding gain from recovering to its initial value when the first pulse exits SOA<sub>1</sub> while  $P_{FBL}$  still has yet to arrive. Similar to the set pulse, a reset pulse, after a delay of  $T_{ON}$  (the on interval), creates *R*, which is applied to the lower control input of the SMZ. The first pulse of *R* saturates the SOA<sub>2</sub> gain dropping it to the same level of SOA<sub>1</sub> saturating gain (i.e., restoring the gain and phase balance between SMZ arms) and once again toggling the AOFF to its off state because cw is no longer switched to *Q*. Note  $P_{FBL}$  is still in the upper control port within a subsequent  $T_{FBL}$  period although there is no output signal at *Q*. To retain the same gain level in both SOAs in this period, the following pulses in *R* will ensure a continuous gain saturating of SOA<sub>2</sub> for the SMZ to be in balance, thus completely turning off the *Q* signal during and after  $T_{FBL}$  once the reset signal is applied.

## 3 AOFF Stability

The temporal gain of the output *Q* is expressed by:<sup>7</sup>

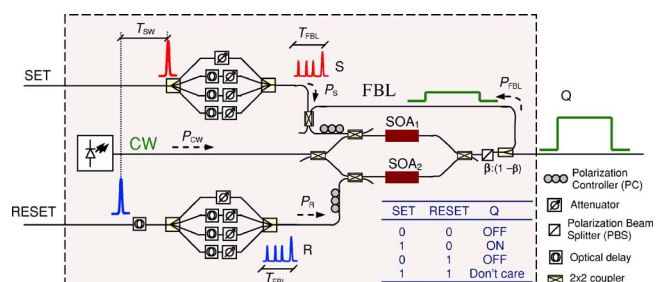


Fig. 1 Multiple forward-control AOFF configuration.

$$Q(t) = K \left( G_1(t) + G_2(t) - 2\sqrt{G_1(t)G_2(t)} \right) \times \cos \left\{ -\frac{\alpha_{LEF}}{2} \ln \left[ \frac{G_1(t)}{G_2(t)} \right] \right\}, \quad (1)$$

where  $K$  is an overall constant coupling factor,  $G_1(t)$  and  $G_2(t)$  are the temporal gain profiles of SOA<sub>1</sub> and SOA<sub>2</sub>, and  $\alpha_{LEF}$  is the SOA linewidth enhancement factor. It is noted that  $Q(t)=0$  when  $G_1(t)=G_2(t)$ . The SOA gain computed over a SOA length  $L_{SOA}$  is given by:<sup>7</sup>

$$G(t) = \frac{P(L_{SOA},t)}{P(0,t)} = \exp \left[ \Gamma g \int_0^{L_{SOA}} N(z,t) \Delta z \right], \quad (2)$$

where  $\Gamma$  is the confinement factor,  $g$  is the gain coefficient, and  $N(t)$  is the SOA carrier density. The gain profiles are, therefore, dependent on the temporal change of carrier, which is governed by the SOA rate equation with the applied average power  $P(t)$  (Ref. 8):

$$\frac{\partial N(t)}{\partial t} = \frac{I_e}{qV_{SOA}} - \frac{N(t)}{\tau_e} - \frac{P(t)g[N(t) - N_T]}{hvA_{SOA}}, \quad (3)$$

where  $I_e$  is the injection dc current,  $q$  is the electron charge,  $V_{SOA}$  is the active volume,  $\tau_e$  is the carrier lifetime,  $hv$  is the photon energy,  $A_{SOA}$  is the cross-section area of the active region, and  $N_T$  is the carrier density at transparency. To achieve operational stability in the AOFF, the feedback power is constrained to match with the average powers of both  $S$  and  $R$  signals. This will ensure the steady imbalance and balance states in SMZ during the transient durations when the AOFF is switched to the on and off states, respectively. These constraints are represented as follows:

$$P_{FBL} = \sum_{m=0}^{M-1} P_{S,avg} \left( t + \frac{mT_{Loop}}{M} \right), \quad (4)$$

$$\sum_{m=0}^{M-1} P_{R,avg} \left( t + \frac{mT_{Loop}}{M} \right) = \frac{P_{FBL}}{2}, \quad (5)$$

where  $P_{S,avg}(t)$  and  $P_{R,avg}(t)$  are the average powers of control pulses in  $S$  and  $R$  streams, respectively, over  $T_{FBL}$ , and  $M$  is the number of pulses in each  $S$  or  $R$ . In Eq. (4), if  $P_{FBL}$  is smaller than the average power of the applied control signal  $S$ , the  $Q$  signal will eventually cease. However, a greater  $P_{FBL}$  will gradually saturate the SOA gain, thus saturating AOFF-output gain. As a result,  $Q$  varies in a large intensity range, which is determined by the intensity variation ratio (IVR) between the minimum and the maximum values of the  $Q$  signal during  $T_{ON}$ . For a complete turning off in the AOFF, the applied average power of the control signal  $R$  is required to be half of  $P_{FBL}$ , ensuring both SOAs receive the same average control power. If this power is different from  $P_{FBL}$ , a residual signal will emerge at the output  $Q$ , which in turn unexpectedly restores the AOFF to the on state again. This residual signal will therefore deteriorate the on/off contrast ratio (CR) at  $Q$ , which is defined by the power ratio of signals in the on and off states.

**Table 1** Simulation and SOA device parameters.

Parameters	Value
Input power $P_{CW}$	0 dBm
Gaussian pulse width	20 ps
Signal wavelength	1554 nm
$P_S$ (peak power of first pulse)	13.5 dBm
$P_S$ (peak power of following pulses)	8.5 dBm
$P_R$ (peak power of first pulse)	10.5 dBm
$P_R$ (peak power of following pulses)	5.5 dBm
SOA linewidth enhancement factor $\alpha_{LEF}$	5
SOA length $L_{SOA}$	0.5 mm
SOA confinement factor $\Gamma$	0.2
SOA carrier density at transparency $N_T$	$1.4 \times 10^{24} \text{ m}^{-3}$
SOA spontaneous emission factor $n_{sp}$	2
DC-bias $I_e$	150 mA
FBL delay $T_{FBL}$	0.2 ns
Splitting factor $\beta$	15%

#### 4 Results and Discussion

The AOFF operation is validated using VPI simulation software. Simulation and SOA device parameters are given in Table 1. Note that the average power of  $S$  is 3 dB greater than  $R$  because  $S$  is reduced by 3 dB when coupled with  $P_{FBL}$  to ensure that the SOAs are excited with the same set/reset powers. The  $T_{FBL}$  is approximated as 0.2 ns, equivalent to a 40-mm optical waveguide FBL.<sup>5</sup> The SOA model is assumed to be polarization-independent, though in practical systems, polarization-gain dependence ( $\sim 1$  to 2 dB) and the imperfect polarization states of the cw and set/reset signals will slightly affect AOFF operation. The flip-flop operation is illustrated in Fig. 2. A series of set and reset single pulses, shown in Fig. 2(a), are applied to the AOFF in a range of  $T_{ON}$  values of 0.1, 0.2, 0.5, 1, 2, and 5 ns. The resultant temporal gain profiles of SOAs corresponding with the set/reset signals are observed in Fig. 2(b). During a period of  $T_{ON}$ , the SOA<sub>1</sub> gain is kept at the same saturation level by both  $S$  and  $P_{FBL}$ . Figure 2(c) displays the AOFF-output waveforms. There are ripples at the leading edge of the  $Q$  output signal in the on state during  $T_{FBL}$  owing to the variation in the SOA<sub>1</sub> gain profile caused by the discrete excitations on SOA<sub>1</sub> by pulses in  $S$ . When the AOFF is switched off, a small residual signal, lasting in  $T_{FBL}$ , still emerges at  $Q$ . This is due to the gain variation of SOA<sub>2</sub> caused by multiple-pulse excitations of  $R$  in contrast to a flat gain profile of SOA<sub>1</sub> maintained by a leftover of

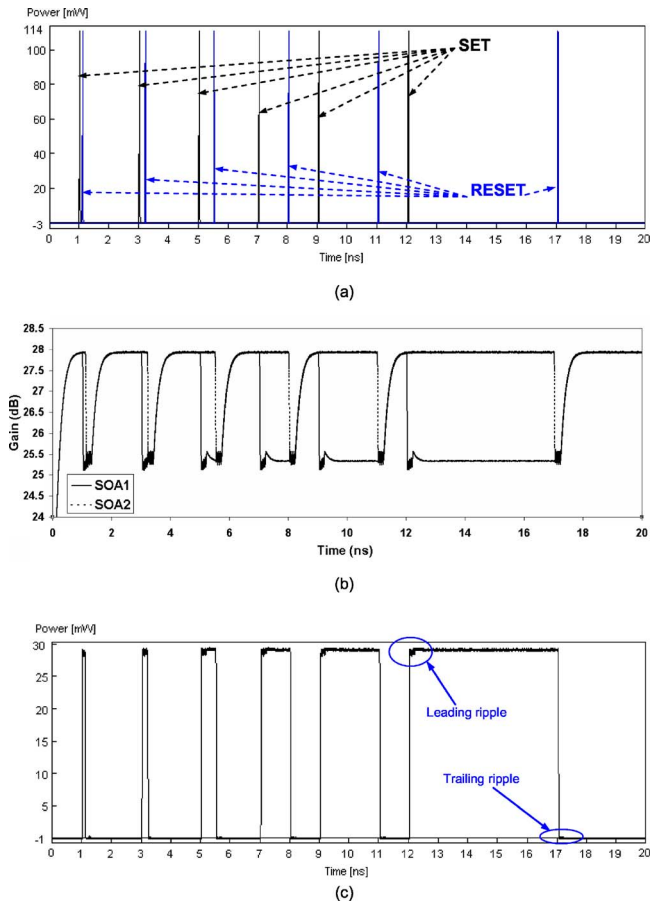


**Fig. 2** (a) Set/reset pulses, (b) temporal gain profiles of SOA<sub>1</sub> and SOA<sub>2</sub>, and (c) AOFF output (*Q*).

constant  $P_{FBL}$  within that  $T_{FBL}$ , hence, causing ripples at the trailing edge of the *Q* signal. It will, therefore, result in on/off CR deterioration.

The graphs in Fig. 3 show that the highest achieved CR is 22 dB at  $\beta=15\%$  [AOFF total output power is 14.5 dB; see Fig. 2(c)] where the conditions in Eqs. (4) and (5) are satisfied at  $T_{ON}=1$  ns. It is also shown that the AOFF output signal is relatively flat during  $T_{ON}$  and the observed IVR is 0.95. Beyond this optimum operation point, both CR and IVR are considerably decreased due to high residual power and improper feedback power, respectively. Note that high  $\beta$  results in flat-level performance in CR and IVR; however, since SOA<sub>1</sub> gain is saturated due to high-power  $P_{FBL}$ , their values are noticeably small.

**5 Conclusions**

A new AOFF configuration based on a SMZ with FBL and multiple-pulse forward set/reset signals is proposed. A mul-

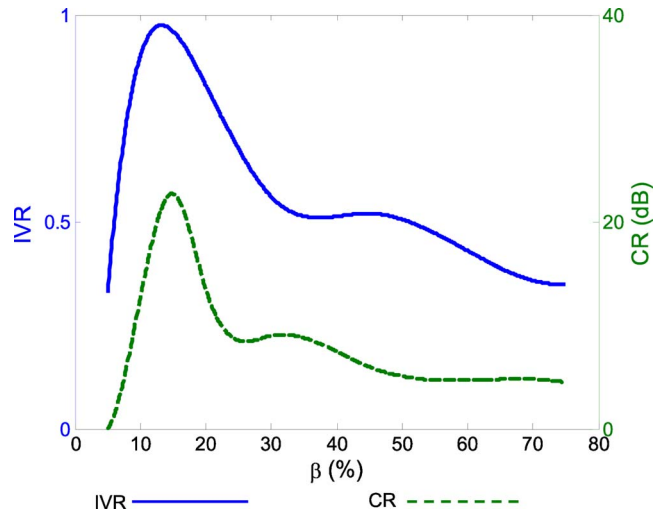


**Fig. 3** AOFF IVR and CR against  $\beta$  (at  $T_{ON}=1$  ns).

iple set/reset control-signal scheme fully overcomes the feedback-loop delay, thus making AOFF suitable for high-speed memory or signal processing applications where  $T_{ON}$  is required to be as small as a few hundred picoseconds regardless of the FBL delay. In addition, the forward controls enhanced the AOFF toggling response within the pulse width of the set and reset signals. On/off contrast and intensity variation ratios of 22 dB and 0.95, respectively, are achieved at the optimum operating point.

**References**

1. F. Ramos, E. Kehayas, J. M. Martinez, R. Clavero, J. Marti, L. Stampoulidis, D. Tsiokos, H. Avramopoulos, J. Zhang, P. V. Holm-Niesen, N. Chi, P. Jeppersen, N. Caenegem, D. Colle, M. Pickavet, and B. R. Ti, "IST-LASAGNE: Towards all-optical label swapping employing optical logic gates and optical flip-flops," *J. Lightwave Technol.* **23**, 2993–3011 (2005).
2. M. T. Hill, A. Srivatsa, N. Calabretta, Y. Liu, H. D. Waardt, G. D. Khoe, and H. J. S. Doren, "1×2 optical packet switch using all-optical header processing," *Electron. Lett.* **37**, 774–775 (2001).
3. M. T. Hill, H. D. Waardt, G. D. Khoe, and H. J. S. Doren, "All-optical flip-flop based on coupled laser diodes," *IEEE J. Quantum Electron.* **37**, 405–413 (2001).
4. M. Takenaka, M. Raburn, and Y. Nakano, "All-optical flip-flop multimode interference bistable laser diode," *IEEE Photonics Technol. Lett.* **17**, 968–970 (2005).
5. R. Clavero, F. Ramos, J. M. Martinez, and J. Marti, "All-optical flip-flop based on a single SOA-MZI," *IEEE Photonics Technol. Lett.* **17**, 843–845 (2005).
6. B. C. Wang, V. Baby, W. Tong, L. Xu, M. Friedman, R. J. Runster, I. Glesk, and P. Prucnal, "A novel fast optical switch based on two cascaded terahertz optical asymmetric demultiplexers (TOAD)," *Opt. Express* **10**, 15–23 (2002).
7. Z. Ghassemlooy and R. Ngah, "Simulation of 1×2 OTDM router employing symmetric Mach-Zehnder switches," *IEE Proc.: Circuits Devices Syst.* **152**, 171–177 (2005).
8. G. P. Agrawal and N. A. Olsson, "Self-phase modulation and spectral broadening of optical pulses in semiconductor laser amplifiers," *IEEE J. Quantum Electron.* **25**, 2297–2306 (1989).